Effect of Vehicles and Penetration Enhancers on the *In Vitro* and *In Vivo* Percutaneous Absorption of Methotrexate and Edatrexate Through Hairless Mouse Skin

Dhruba J. Chatterjee,[1,3] Wen Y. Li,[2] and Robert T. Koda[2]

Received March 13, 1997; accepted May 21, 1997

Purpose. Low-dose methotrexate (MTX) is approved for the treatment of recalcitrant rheumatoid arthritis (RA). The objective of this study was to determine the effect of vehicles and penetration enhancers on the percutaneous absorption of MTX and its analog edatrexate (EDAM), and develop transdermal (TD) delivery systems of the drugs for the treatment of RA.

Methods. From previously published pharmacokinetic parameters with low-dose MTX therapy, and considering a 50 cm^2 diffusional area, the target steady state *in vitro* TD flux for MTX was calculated to be 35 $\mu g/cm^2/hr$. Modified Franz diffusion chambers and hairless mouse skin were used for *in vitro* skin permeation studies. Hairless mice were used for *in vivo* studies. Delivered amounts of MTX and EDAM were determined by assaying the receiver phase fluid (or blood) with validated reversed phase HPLC methods.

Results. Intrinsic partition coefficient of MTX was low (log P = −1.2). Target MTX fluxes of ≥ 35 $\mu g/cm^2/hr$ were achievable only with 1–15% (v/v) Azone® in propylene glycol (PG). Flux of EDAM (85 $\mu g/cm^2/hr$) was higher than MTX from an isopropyl alcohol (IPA)—5% (v/v) Azone® system. Clinically significant steady state *in vivo* blood concentration of MTX and EDAM was achieved using delivery systems containing ≥ 2.5% Azone® in PG. Area under the drug concentration-time curves (AUC_{0-24hr}) for MTX were 2379 and 3534 ng*hr/ml from PG—2.5% Azone® and PG—7.5% Azone® systems respectively. AUC_{0-24hr} of EDAM was 6893 ng*hr/ml using a PG—2.5% Azone® system.

Conclusions. Results of this study show the feasibility of using a transdermal delivery system of MTX and EDAM for the treatment of rheumatoid arthritis.

KEY WORDS: methotrexate; edatrexate; transdermal; percutaneous; rheumatoid arthritis.

INTRODUCTION

Methotrexate (MTX) was introduced in 1948 and still remains the most widely used compound in the antifolate class of antineoplastic agents. Other than its use at high doses for treating several types of carcinoma, low-dose MTX has been frequently employed as an immunosuppressant in the treatment of psoriasis and rheumatoid arthritis (RA). Its use in RA has been firmly established since the 1960s (1–6). In 1988, MTX was approved by the FDA for use in patients with severe RA, refractory to conventional therapy.

An inherent problem with MTX therapy in RA from conventional doses has been toxicity, precluding its use as the first line of therapy along with NSAIDS. Gastrointestinal (GI) toxicity (abdominal cramping, nausea, vomiting, diarrhea), cytopenia, pulmonary toxicity, hepatic toxicity, stomatitis, alopecia are most common (6–10). Oral administration leads to GI toxicity, intravenous (IV) route results in systemic toxicity, and intraarticular administration is painful. Subcutaneous and intramuscular routes showed improved results as compared to IV dose due to completeness of drug absorption in comparison to oral dosing (11). Moreover, high potency of MTX in RA (7–15 mg per week), the chronic nature of disease, a short MTX $t_{1/2}$ (4–5 hr), and inter & intrapatient variability strongly supports a rationale to develop a transdermal delivery system of MTX for the treatment of severe and recalcitrant RA.

Literature documenting the topical use of MTX in the treatment of psoriasis were focused primarily on MTX pharmacology and delivery into the epidermal layer of skin (12–14). Few other *in vitro* studies evaluated the effect of pH, vehicles, penetration enhancers, prodrug, and analogs on the delivery of MTX to the different skin tissues and across hairless mice, rat, and human skin (15–20). The percutaneous flux for MTX obtained was considerably lower than that required for use against RA. There is no literature available focusing on the role of individual factors that might contribute to the skin permeation and systemic delivery of MTX suitable for a specific therapeutic need. A more recent study indicated that an analog of MTX, edatrexate (EDAM), might be more effective and less toxic in the treatment of RA (21).

This study systematically evaluated the role of vehicles and penetration enhancers towards achieving a steady state flux of methotrexate and edatrexate therapeutically significant against rheumatoid arthritis. Both *in vitro* and *in vivo* results are reported.

MATERIALS AND METHODS

Chemicals and Supplies

(±)Amethopterine (methotrexate), aminopterine, propylene glycol (PG), polyethylene glycol 400 (PEG 400), isopropanol (isopropyl alcohol, IPA), dimethyl sulfoxide (DMSO), *N*-octanol, 1-monocapryloyl-rac-glyceryl (GMC), and p-(N-2,4-diaminopteridinylmethyl-N-methylamino)benzoic acid were obtained from Sigma Chemical Co. (St. Louis, MO). Edatrexate was obtained as a gift from the laboratory of Dr. Collin P. Spears' of Norris Comprehensive Cancer Hospital (Los Angeles, CA). β-cyclodextrin hydrate (β-CD) and hydroxypropyl-β-cyclodextrin (HP-β-CD) were obtained from Aldrich Chemical Co. (Milwaukee, WI). Azone® (1-dodecylazacycloheptan-2-one, Laurocapram), was obtained as a gift from Syntex Research (Palo Alto, CA). *N*-decylmethyl sulfoxide was purchased from Narchem Chemical Co. (Chicago, IL). HPLC solvents (methanol, acetonitrile) were obtained from Baxter Scientific Products (Irvine, CA). Solid phase extraction columns (C_{18}, 200 mg) for analytical sample preparation were purchased from Baxter Healthcare Co. (Muskegon, MI). Hill Top Chambers® (transdermal application devices) were purchased from Hill Top Compa-

[1] College of Pharmacy Rm. 2059, University of Michigan, 428 Church Street, Ann Arbor, Michigan 48109.

[2] School of Pharmacy, Rm 200C, University of Southern California, 1985 Zonal Avenue, Los Angeles, California 90033.

[3] To whom correspondence should be addressed. (e-mail: dhruba@umich.edu)

0724-8741/97/0800-1058$12.50/0

nies (Cincinnati, OH). All other chemicals were of reagent grade and used without further purification.

Animals

Hairless mice (strain HRS/JR) of ages 8–10 weeks were obtained from Charles River Breeding (Wilmington, MA) and used for *in vitro* and *in vivo* studies. The body weight of the animals varied between 20–30 gm.

HPLC Assay of MTX and EDAM

High performance reversed phase liquid chromatographic method with a Beckman Ultrasphere C_{18} analytical column (250 × 4.6 mm; 5μ) was used to analyze the concentration of MTX and EDAM in samples. For MTX, the mobile phase consisted of 0.1 *M* sodium phosphate (monobasic) and 0.1 *M* tris hydrochloride in 23% methanol (v/v). Mobile phase for the EDAM assay consisted of 10 mM ammonium formate buffer in 45% methanol (v/v) containing 1g/L of tetramethyl ammonium chloride. Samples were analyzed using UV detection at 303 and 350 nm for MTX and EDAM respectively. The internal standards were aminopterine for MTX and p-(N-2,4-diaminopteridinylmethyl-N-methylamino)benzoic acid for EDAM. The flow rate of the solvent pump was set at 1.5 ml/min. For aqueous solutions with low drug concentrations (<100 ng/ml) and all plasma samples, a solid phase extraction (SPE) method was used for sample preparation. Following SPE, the drug was eluted with methanol, dried at 40°C under nitrogen gas, reconstituted in mobile phase and injected into the HPLC system.

The concentration of MTX in *n*-octanol was determined with the help of a UV Spectrophotometer (Shimadzu UV 2101 PC). A linear standard curve was constructed using MTX concentrations in the range 2.0–20.0 ng/ml, and the unknown concentrations were determined using the standard curve as reference.

Partition Coefficient (K)

Partition coefficients were determined by shaking (overnight) the aqueous phase containing a known concentration of MTX with *n*-octanol. Next, the phases were allowed to separate and each of the two phases were assayed for MTX. K_{oct} was calculated as the ratio of MTX concentration in *n*-octanol to that in the aqueous phase. All partition coefficients were determined at room temperature.

Skin Penetration Studies (*In Vitro*)

Hairless mice were sacrificed and the skin was separated. Subcutaneous fat was carefully removed and circular skin segments were mounted between the donor and receiver compartments of modified vertical Franz diffusion cell apparatus (stratum corneum side facing the donor). For some experiments, skin samples were stripped repeatedly (25 times) with Scotch Tape® (3M, Minneapolis, MN). The area of diffusion for all *in vitro* experiments was 1.8 cm^2. The receiver compartments were filled (~12 ml) with an isotonic phosphate buffer solution (pH = 7.4, preserved with 0.002% gentamicin as an antibacterial agent). The receiver phase was stirred constantly and its temperature was maintained at 37°C. Skin segments were allowed to equilibrate with the receiver phase for 30 min before charging each donor compartment (3 ml) with drug formulations. At predetermined time intervals (starting with a blank sample), 1.5 ml of the receiver compartment was withdrawn for drug analysis and replaced with the same volume of blank receiver buffer. At the beginning of each experiment, donor solutions were also assayed for drug concentration.

Data Analysis and Calculations

Data analysis was performed according to the following Fick's Law equations:

$$(1/A) \cdot (dM/dT) = J_{ss} = P \cdot (C_d - C_r) \cong P \cdot C_d$$

$$P = (K \cdot D)/L; \text{ and } T_{lag} = L^2/6D$$

where dM/dT is the steady state slope (μg/hr), J_{ss}, the steady state flux (μg/cm^2/hr), P, the effective permeability coefficient (cm/hr), A, the effective drug diffusion area, C_d and C_r, the drug concentrations (μg/ml) in the donor and receiver compartments, respectively. In almost all experimental cases, C_d is the solubility of the drug in the vehicle. K is the partition coefficient of the drug between vehicle and skin, L (cm), the thickness of skin, T_{lag} (hr), the lag time for steady-state drug diffusion and D (cm^2/sec), the apparent diffusivity for the steady-state diffusion of the drug through skin. The *in vitro* skin permeation data obtained were plotted as the cumulative amount of drug penetrated into the receiver phase as a function of time. The slope of the straight line portions of this plot (at steady state) yielded the values of flux (J). Lag times were determined by extrapolating these straight lines to the X-axis .

Previous studies involving low dose MTX in RA patients reported the pharmacokinetic parameters of the drug (11,22–24). Assuming MTX Cp_{ss} (steady state plasma concentration) of 0.5 μg/ml for the treatment of RA, a required zero order delivery rate (K_0) could be calculated from previously reported parameters:

$$K_0 = Cp_{ss} \cdot k_{el} \cdot V_d$$

$$= (0.5 \text{ μg/ml}) \cdot 0.154 \text{ (hr}^{-1}\text{)} \cdot (23000 \text{ ml})$$

$$= 1771.0 \text{ μg/hr;}$$

Therefore, for a transdermal patch of 50 cm^2 area, the *in vivo* transdermal flux adequate to maintain the desired Cp_{ss} is ≅ 35 μg/cm^2/hr.

Animal Experiments (*In Vivo*)

Drug solutions were prepared by shaking excess drug in the solvents overnight and then centrifuging the suspension. 0.2 ml of the clear supernatant was loaded into each Hill Top Chamber® (total diffusion area 0.95 cm^2). The drug-loaded Hill Top Chamber® was attached to the back of each mouse and held in place by adhesive surgical tape. The chambers remained in place throughout the experiment (24 hr). At predetermined time points (1, 2, 3, 6, 9, 12, and 24 hr) following device application, blood samples (1 ml) were collected by cardiac puncture under ether anesthesia into pre-heparinized centrifuge tubes (n = 4 or 5 mice per time point). Plasma was separated and frozen until HPLC assay. Following analysis, drug concentration was plotted against time (linear plot) and pharmacokinetic parameters T_{max} (time to achieve maximal plasma

concentration), C_{max} (maximal plasma concentration), Cp_{ss} (steady state plasma concentration), and AUC_{0-24hr} (area under the curve between 0–24 hr) were determined.

RESULTS

Assay Validation of MTX

Following six runs of MTX standard curves on different days, the composite standard curve was obtained. The mean (±s.d.) slope and Y-intercept were 0.007 (±0.0007) and 0.009 (±0.005) respectively. The correlation coefficient of this composite line indicated that the assay was linear (R^2 = 0.999). Within and between-run validation results were determined and all the values for precision and accuracy were within ±5%. The limit of detection was 2.5 ng of MTX injected. Validation of the analytical method proved that the analysis was acceptable in terms of reproducibility, precision, linearity, and accuracy.

Physicochemical Properties

MTX (Figure 1a) is a polar compound due to the presence of a glutamic acid moiety in its structure. It has a pKa of 4.7 and its solubility in pH 4.0 buffer was low (0.32 g/L). Table I shows the solubility of MTX determined in various solvents. To increase the intrinsic aqueous solubility of MTX, large molecular solubilizing agents cyclodextrin (CD) and derivative hydroxypropyl-β-cyclodextrin (HP-β-CD) were used. Even at high (20%) HP-β-CD concentration, the solubility of MTX was 2.8 g/L. EDAM (Figure 1b) was freely soluble in PG (>17.0 g/L). Its solubility in IPA and EtOH were 0.060 g/L and 0.095 g/L respectively.

LogK_{oct} of MTX from pH 4.0 buffer, 1.5% β-CD, 10% HP-β-CD, and 20% HP-β-CD were determined to be −1.23, −1.90, −2.40, and −2.60 respectively. This confirmed the polarity of MTX, and also the increasing affinity of the drug

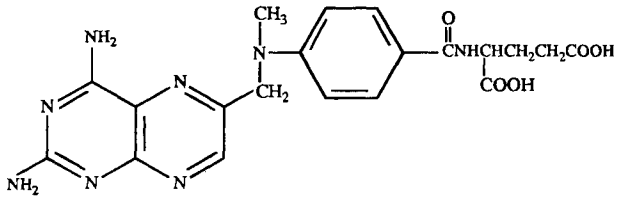

(a)

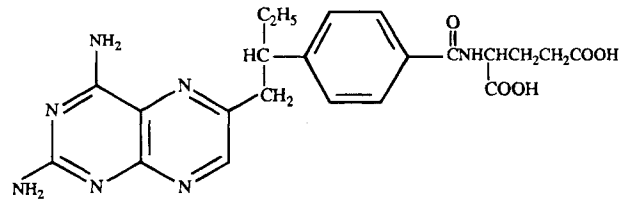

(b)

Fig. 1. Chemical structures of (a) methotrexate (MTX) and (b) edatrexate (EDAM).

Table I. Solubility, Partition Coefficient, and Solubility Ratios of MTX in Different Solvents

Solvent Systems	S (g/L)	LogK_{oct}	S^a_{oct}/S_v
pH = 4.0 buffer	0.320	−1.23	0.031
10% PG	0.420	N. D	0.024
60% PG	0.260	N. D	0.038
100% PG	4.800	N. D	0.002
1.5% β-CD	0.800	−1.90	0.013
10% HP-β-CD	1.600	−2.40	0.006
20% HP-β-CD	2.800	−2.60	0.004
10% DMSO	0.220	N. D	0.045
60% DMSO	1.080	N. D	0.009
100% DMSO	6.450	N. D	0.002
10% PEG 400	0.200	N. D	0.050
60% PEG 400	0.820	N. D	0.012
100% PEG 400	4.600	N. D	0.002
100% IPA	0.060	N. D	0.167
100% EtOH	0.095	N. D	0.105
100% *n*-octanol	0.010	—	—

[a] Ratio of MTX solubility in *n*-octanol to same in each vehicle. N.D.—not determined.

for the different solutions in the order as mentioned above. PG, PEG 400, DMSO, EtOH, and IPA being partially or fully miscible with *n*-octanol, the partition coefficient of MTX could not be determined for these solvents. Instead, the ratios of solubility of the drug in *n*-octanol to that in each vehicle were evaluated. This ratio indicated the relative magnitude of the "escaping tendency" of the drug from the vehicle to *n*-octanol. According to the S_{oct}/S_v ratio (Table I), MTX was expected to show the highest escaping tendency from 100% IPA (S_{oct}/S_v = 0.167), and the lowest from 100% DMSO (S_{oct}/S_v = 0.0016). A plot of the partition coefficient (whichever determined) against the solubility ratio produced a straight line (R^2 = 0.966). A theoretical estimation of the partition coefficient of MTX from each indeterminable vehicle could be made from this plot using the respective S_{oct}/S_v values (results not shown).

In Vitro Skin Penetration Studies

Effect of Solvents

Table II summarizes the skin permeation parameters of MTX from a majority of the formulations evaluated experimentally. The values of J_{ss}, P and T_{lag} (lag time) are reported against the respective delivery vehicle. The highest mean J_{ss} was obtained with IPA as the solvent (3.04 μg/cm²/hr), followed by EtOH, 20% DMSO, 5% DMSO, PG, and pH 4.0 buffer. The lowest flux was obtained with PEG 400 (0.003 ± 0.001 μg/cm²/hr). The value of P was in the order of 10^{-2} cm/hr with IPA and EtOH, 10^{-5} with DMSO, 10^{-6} with PG, and 10^{-7} cm/hr with PEG 400. T_{lag} followed a similar trend. The highest T_{lag} was obtained using PEG 400 (18.0 ± 5.0 hr). Lag times were lower with IPA (9.4 ± 1.0 hr) and EtOH (4.7 ± 1.5 hr).

Effect of Penetration Enhancers

Penetration enhancers were utilized to enhance the intrinsic skin permeability of MTX. The agents used were 0.1%, 0.5%, 1%, 5%, and 10% NDMS (*n*-decylmethyl sulfoxide), 1%, 2.5%,

Table II. Skin Permeation Parameters (Flux, Permeability, and Lag Times) of MTX from Different Formulations Across Hairless Mouse Skin

Delivery systems[a]	J_{ss}[b] (μg/cm²/hr)	P[b] (cm/hr)	T_{lag}[b] (hr)
Phosphate Buffer (pH = 4.0)	0.006±0.004	$(5.0\pm3.6)\times10^{-6}$	16.3±1.3
100% PEG 400 (n = 2)	0.003±0.001	$(1.6\pm1.0)\times10^{-7}$	18.0±5.0
100% PG (n = 6)	0.016±0.014	$(2.3\pm2.6)\times10^{-6}$	14.2±3.6
100% IPA	3.04±1.19	$(5.1\pm2.0)\times10^{-2}$	9.4±1.0
100% EtOH	1.59±0.49	$(1.7\pm0.5)\times10^{-2}$	4.7±1.5
5% DMSO in PG (v/v)	0.097±0.020	$(1.8\pm0.36)\times10^{-5}$	12.8±2.0
20% DMSO in PG (v/v)	0.144±0.025	$(2.3\pm0.36)\times10^{-5}$	10.3±2.6
1% NDMS in PG (w/v)	0.119±0.080	$(1.2\pm0.79)\times10^{-4}$	3.8±3.2
10% NDMS in PG (w/v)	0.225±0.140	$(3.4\pm2.1)\times10^{-5}$	6.8±1.0
3% Azone® in IPA (v/v)	17.6±4.9	$(6.4\pm1.8)\times10^{-1}$	7.24±3.8
5% Azone® in EtOH (v/v)	8.7±5.3	$(8.0\pm4.8)\times10^{-2}$	6.09±1.8
3% Azone® in PO^{2-4} buffer (pH = 7.4)	5.72±0.50	$(2.1\pm0.19)\times10^{-2}$	7.5±3.3
0.1% Azone® in PG (v/v)	0.010±0.010	$(3.4\pm3.4)\times10^{-6}$	10.3±0.6
1% Azone® in PG (v/v) (n = 2)	35.7±23.8	$(9.0\pm6.0)\times10^{-3}$	9.4±1.3
5% Azone® in PG (v/v)	61.6±25.8	$(1.6\pm0.7)\times10^{-2}$	3.7±0.8
10% Azone® in PG (v/v)	71.4±18.0	$(1.8\pm0.4)\times10^{-2}$	3.2±0.9
15% Azone® in PG (v/v)	64.4±8.9	$(1.6\pm0.2)\times10^{-2}$	3.0±0.3
10% GMC in PG (w/v)	0.08±0.03	$(9.7\pm3.2)\times10^{-5}$	7.9±4.1
2% GMC + 2% Azone® in PG (w/v/v) (n = 2)	13.7±0.78	$(1.4\pm0.8)\times10^{-2}$	13.2±3.6
5% Azone® in 50% PG + 45% water (v/v/v)	4.3±2.0	$(5.5\pm2.6)\times10^{-3}$	5.5±0.4
5% Azone® + 5% DMSO in 45% PG + 45% water	5.4±2.9	$(6.3\pm3.3)\times10^{-3}$	5.5±0.8
100% PG [skin—stripped 20 times with Scotch Tape®]	44.2±2.3	$(3.1\pm0.16)\times10^{-2}$	1.3±1.2

[a] n = 3, unless otherwise mentioned.
[b] Expressed as mean±s.d.

5%, 10% GMC (glyceryl monocaprylate), and 0.1, 0.5, 1.0, 5.0, 10.0, and 15.0% (v/v) of Azone® (all in PG). Azone® was the most effective in enhancing flux and permeability of MTX. The maximal achievable flux of MTX (mean ± s.d) with 10% NDMS, and 10% GMC in PG were 0.225 ± 0.14, 2.19 ± 0.91 and 0.08 ± 0.03 μg/cm²/hr, respectively. In comparison, the highest flux of MTX achieved with 10% Azone® in PG was 71.4 ± 18.0 μg/cm²/hr. Use of Azone® resulted in higher values of MTX permeability and reduced lag times in comparison to the other agents. IPA, EtOH and phosphate buffer (pH = 4.0) containing MTX and 3.0%, 5.0% and 3.0% Azone® respectively, resulted in flux considerably lower than that achieved with PG as the solvent and Azone® at similar concentrations. The flux of MTX from a formulation containing MTX in neat PG across stripped skin was 44.2 ± 2.3 μg/cm²/hr. Figure 2(a) describes the skin permeation profile of MTX from PG-Azone® systems, and Figure 2(b) shows the relationship between MTX flux and Azone® concentration.

Solvent and Penetration Enhancer Combinations

Among the combinations evaluated were 50% PG (in water) containing 5% Azone®, 5% DMSO in 45% PG (in water) and 5% Azone®, 1% GMC and 1% Azone® in PG, and 2% GMC and 2% Azone® in PG. The flux of MTX from these were appreciably lower than the target value of 35.4 μg/cm²/hr (Table II). The solvent system and penetration enhancer combinations had neither the additive, nor synergistic effects on MTX transdermal flux. Figure 3 graphically summarizes the results of a majority of the skin permeation experiments with MTX.

Skin Permeation of EDAM

Suspensions of EDAM in 100% PG, 1% Azone® in 99% PG, 5% Azone® in 95% PG, and 5% Azone® in 95% IPA were evaluated for skin flux. Results are summarized in Table III. EDAM flux from a 5% Azone® system in 95% PG was low. The flux achieved using 5% Azone® in 95% IPA was substantially higher than the target flux calculated for MTX. Unlike MTX, the target flux for EDAM could not be calculated since the effective plasma concentration of EDAM in RA has not yet been reported.

In Vivo Skin Penetration Studies

In vivo experiments were performed following transdermal application of vehicles with MTX in PG containing 7.5% and 2.5% Azone®, and with EDAM from its solution in PG containing 2.5% Azone®. For each time point, 4–5 mice were sacrificed. The pharmacokinetic profiles are shown in Figure 4. T_{peak}s were achieved within 2–3 hours of device application. C_{max} values for MTX were 260 and 170 ng/ml from the 7.5% and 2.5% Azone® formulations respectively. Steady state concentration of MTX in blood was achieved 6 hr post application from both the formulations. The plasma concentration of MTX was sustained for 24 hr from the 7.5% Azone® formulation, but was not sustained beyond 12 hr from the 2.5% Azone® formulation. The steady state concentration of MTX from the latter was between 125 and 150 ng/ml. AUC_{0-24} for MTX was 3534.0 and 2378.6 ng*hr/ml from the 7.5% and 2.5% Azone® formulations respectively. For EDAM, the value of C_{max} was close to 270 ng/ml with a T_{peak} = 3 hr. Steady state plasma

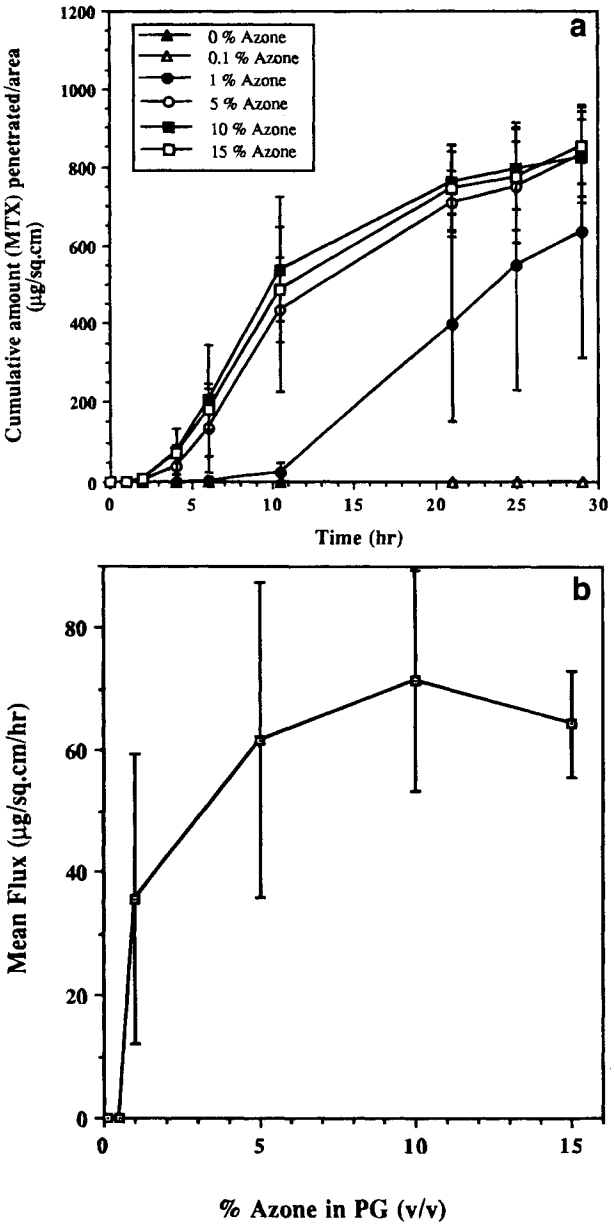

Fig. 2. (a) *In vitro* permeation profile of MTX across hairless mouse skin from formulations containing different concentrations of Azone® in propylene glycol, and (b) relationship between skin flux of MTX and increasing concentrations of Azone® in propylene glycol.

concentrations varied between 270 and 320 ng/ml. The plasma concentration of EDAM from the transdermal device was sustained till 24 hr with an AUC_{0-24} of 6892.6 ng*hr/ml.

Following each experiment, the Hill Top Chambers® were removed and the drugs remaining in them were analyzed. The difference between the drug amount initially loaded and the amount after each time point equaled the amount of drug that disappeared from the patches till that time point. The disappearance of MTX and EDAM from the patches were plotted against time and the plots were linear (25).

DISCUSSION

Intrinsic MTX flux values obtained in this study involving either pure solvents or aqueous buffer were in the same range (ng/cm^2/hr) as reported earlier. Aungst *et al.* reported MTX percutaneous flux of 7.0 µg/cm^2/hr across human cadaver skin *in vitro* from neat PG (20). Human skin is known to be approximately ten times less permeable compared to hairless mice skin for a wide variety of drugs. To our knowledge, this was the only instance when a compound having an octanol-water partition coefficient lower than 0.01 showed intrinsic flux in the range of µg/cm^2/hr across human skin. Our results differed considerably. In all other previous reports (15–19), the skin flux of MTX achieved was considerably lower than the therapeutic target reported in this study for rheumatoid arthritis.

To improve the solubility of MTX in the vehicle, different solvents and cosolvent systems were utilized. Solubility of MTX was highest in PG, DMSO, and PEG 400. Lower solubilities were obtained with high concentration (20%) of HP-β-CD and CD. Solubility of MTX was lower with EtOH, IPA, and *n*-octanol. Among these solvents, DMSO is not a practical vehicle due to its toxicity to the skin (26). The *in vitro* skin permeation of MTX from PEG 400 was the lowest, possibly because of a higher degree of interaction of MTX with the polymer leading to a low diffusion coefficient. Skin permeation of MTX from EtOH and IPA was considerably higher than that compared to PG. However, PG was preferred as the solvent for MTX over IPA and EtOH due to its higher solubility for the drug and considerably lower volatility as a solvent compared to the latter two.

Low fluxes and partition coefficients of MTX from solvents having higher drug solubility indicated a need for an increase in drug diffusivity though skin. Penetration enhancers were used for this purpose. Among all enhancers used, the maximal and target skin flux was only achieved using Azone®. Azone® is one of the series of *n*-alkylated cyclic amides with a high degree of lipophilicity (partition coefficient 6.2). The chemical structure of Azone® is highlighted by a polar lactam ring and a long hydrophobic alkyl side chain. The mechanism of action of Azone® is primarily due to its capability to interact with the polar regions (lactam ring) as well as the structural lipids (long alkyl chain). Three skin lipid transition temperatures (T1, T2, T3) completely disappear in the presence of Azone®, while the fourth (T4) remains unaffected. This implies that Azone® action is limited to the extracellular structured lipids and has almost no action intracellularly (27).

PG has been extensively used as a solvent for transdermal and topical formulations. Besides acting as a solvent for various compounds leading to an increased thermodynamic activity and enhanced "solvent drag" of the drug molecule, PG is also believed, at least partially, to act as a penetration enhancer remaining within the cells and intercellular spaces (28). Okamota *et al.* evaluated the role of solubility parameter as a factor in governing skin flux and permeability of acyclovir (a polar compound) (29). They concluded that the enhancer potential was maximum using a vehicle with highest solubility parameter in combination with a penetration enhancer with the lowest solubility parameter. This study showed a maximum flux of acyclovir using a combination of PG and Azone®. In the current studies with MTX, PG had the highest solubility parameter (14.8 cal/cm^3)$^{1/2}$ among the solvents. Azone® had the lowest solubility parameters among the penetration enhancers [9.07 (cal/cm^3)$^{1/2}$] and the maximal enhancement effect on MTX skin penetration using PG as the vehicle. Consideration of solubility

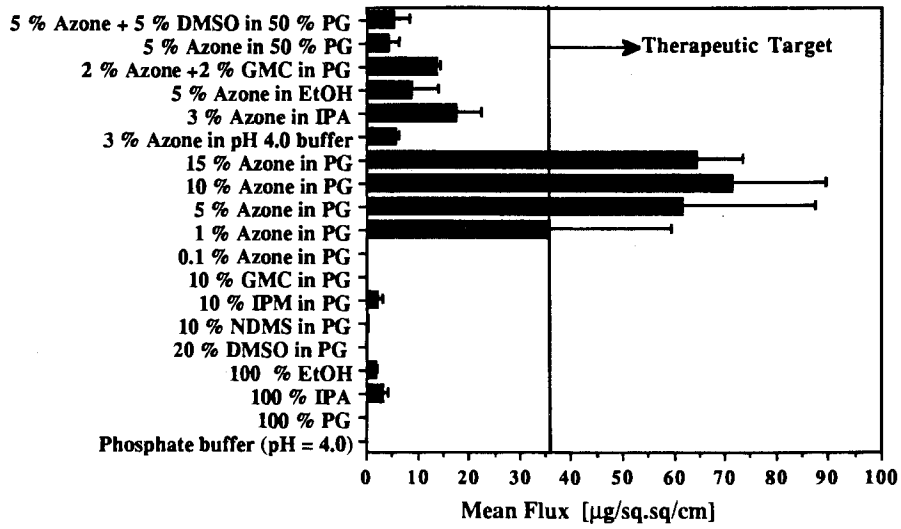

Fig. 3. Composite graph comparing the *in vitro* flux of MTX achieved from different formulations with respect to the therapeutic target.

parameters was a key factor in selecting PG as the solvent for MTX skin permeation.

Synergism of skin flux with PG in combination with Azone® was previously reported by other researchers (30). Azone® enhances intercellular drug diffusion and intracellular proteins offering considerable resistance to drug permeation, are not affected by it. PG does not completely penetrate the cells (corneocytes), stays in the intercellular spaces dehydrating intracellular protein structures due to its hygroscopicity and competes with water for hydrogen bonding sites. In combination with Azone®, PG gains access to the intercellular lipids and might occupy hydrophilic regions therein. Conversely, Azone® being solubilized in PG, partition more readily into the intercellular domain. In the presence of high concentrations of Azone® and PG, the intercellular leaflet structure may break down completely leading to formation of globular micelles dispersed in a continuous phase of solvent. The horny stratum corneum can thus transform to a membrane that is sufficiently permeable (27). This mechanism can explain the significant enhancement of MTX flux through skin from formulations containing Azone® in PG.

The maximal steady-state MTX flux achieved through hairless mouse skin *in vitro* was with 10% (v/v) Azone® in PG. Increasing Azone® concentration (1–15%) resulted in an increase in MTX flux. Beyond an apparent "optimum" Azone® concentration (10% v/v), the flux of MTX did not increase further (Figure 2b). Compared to a mean MTX flux of 0.02 µg/cm²/hr in 100% PG, the maximum flux obtained using a 10% solution of Azone® in PG was 71.4 µg/cm²/hr, a 3500 fold enhancement. The permeability coefficient of MTX increased from the order of 10^{-6} cm/hr with pure PG to 10^{-2} cm/hr with ≥ 1% Azone® in PG. Lag times reduced from 14.2 hr to 3.2 hr.

To evaluate the relative contributions of PG and Azone® in the enhanced skin flux of MTX, additional experiments was performed. A vehicle containing 3.0% Azone® in phosphate buffer (pH = 4.0) showed an MTX flux of 5.7, almost 1000 times higher than that obtained without the use of Azone®, thus proving a major role of Azone® in enhancing the percutaneous flux of MTX. Across stripped skin from neat PG, MTX flux and permeability coefficient was in the same range as that obtained with ≥1% Azone® in PG across intact skin. The lag time observed across stripped skin was the lowest. This observation, along with the flux values confirmed that the main barrier to the skin permeation of MTX was the stratum corneum, and that Azone® had almost the same effect on MTX permeation as would be seen across skin without stratum corneum (SC). The low standard deviation in the flux and permeability values of MTX following the stripped skin experiment suggested that higher variation in the results from other experiments might have resulted from the structural heterogeneity in the SC of different skin specimens.

In vivo experiments results show that with a higher concentration of Azone® (7.5 % in PG), prolonged delivery of MTX was achieved from the skin depot leading to a sustained steady state plasma MTX concentration till 24 hr. AUC_{0-24h} of MTX from 7.5% Azone® in PG was 1.5 times higher than that obtained with the 2.5% Azone® formulation. For the *in vivo* experiment with EDAM, PG was used as the vehicle although *in vitro* results showed a higher flux from IPA. This was because solubility of EDAM in IPA was low (0.060 g/L). Moreover, IPA being a volatile solvent, the drug permeation profile would

Table III. Skin Permeation Parameters (Flux, Permeability, and Lag Times) of EDAM from Different Formulations Across Hairless Mouse Skin

Delivery systems[a]	J_{ss}[b] (µg/cm²/hr)	P[b] (cm/hr)	T_{lag}[b] (hr)
100% PG	0.221±0.18	$(1.3\pm1.0)\times10^{-5}$	23.2±5.0
1.0% Azone® in PG	4.4±2.12	$(1.2\pm0.6)\times10^{-3}$	4.4±2.1
5.0% Azone® in PG	3.4±0.43	$(2.7\pm1.1)\times10^{-3}$	3.8±3.2
5.0% Azone® in IPA	85.0±26.4	$(4.2\pm1.3)\times10^{-1}$	5.2±4.3

[a] n = 3.
[b] Expressed as mean±s.d.

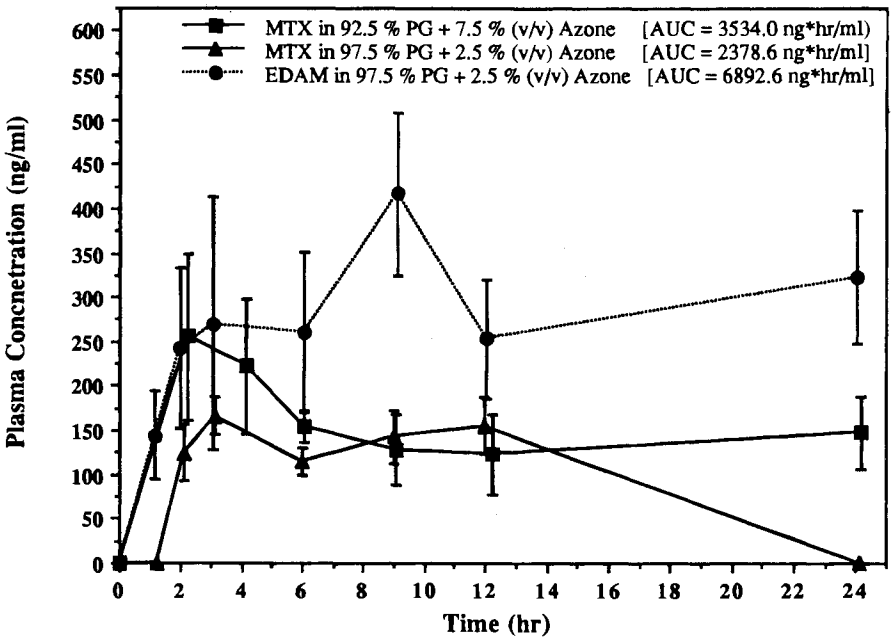

Fig. 4. *In vivo* plasma concentration—time profile of MTX and EDAM in hairless mice following administration of Hilltop Chambers containing transdermal vehicles. Formulations contained varying concentrations Azone® (as indicated) in propylene glycol. For each time point (n = 3 or 4), the mean concentration was plotted, and the s.d. was represented by error bars.

have been affected by the immediate disappearance of solvent from the applied chambers. EDAM was freely soluble in PG. The steady state plasma concentration of EDAM was achieved within 3–4 hours of device application, and this value was 2 times that of MTX from a similar formulation (≅ 250 ng/ml). Plasma drug concentration was prolonged till 24 hr.

EDAM is lipophilic in comparison to MTX. The prolonged delivery of MTX from the 7.5% Azone® system was probably due to a more prolonged residence of an optimum amount of Azone® within the skin layers. In contrast, from the 2.5% Azone® system, the amount of Azone® as well as the MTX depot within the SC was inadequate to achieve the optimal driving force of the drug through the skin for a period ≥ 12 hr. For EDAM, although the concentration of Azone® was 2.5%, higher drug solubility in PG and higher lipophilicity was adequate to maintain the driving force through the skin layers from the depot for a longer period. This explained the prolonged plasma concentration of EDAM. The $AUC_{0-24\ hr}$ for EDAM was 3 times higher than MTX from an exactly similar formulation (2.5% Azone® in PG), and 2 times higher than MTX from the 7.5% Azone® system.

Results of this study indicate that alteration of diffusion coefficient of MTX was a more important factor in governing its flux as compared to an increase in its solubility in the vehicle, or alteration of partition coefficient. Azone® was the most effective skin penetration enhancer for MTX. The research presented in the paper indicates that alteration of physicochemical properties of the delivery vehicle and with the use of a suitable penetration enhancer, a transdermal delivery system of therapeutic significance may be developed for even a relatively polar drug. A preliminary and feasible transdermal vehicle for MTX and EDAM is now available that may be effective in the treatment of rheumatoid arthritis, and can possibly be employed as the first line of therapy against this disease.

ACKNOWLEDGMENTS

The authors would like to sincerely thank the laboratory of Dr. Vincent H. L. Lee for miscellaneous technical assistance.

REFERENCES

1. R. Gubner, S. August, and V. Ginsberg. *Am. J. Med. Sci.* **22**:176–182 (1951).
2. R. B. Rees, J. H. Bennett, and H. L. Arnold. *Arch. Dermatol* **95**:2–11 (1967).
3. R. F. Willkens, M. A. Watson, C. S. Paxon. *J. Rheumatol.* **7**:501–505 (1980).
4. W. S. Wilke, L. H. Calabrese, and A. L. Scherbel. Pilot study. *Clev. Clin. Q.* **47**:305–309 (1980).
5. R. T. Hoffmeister. Oral gold therapy in rheumatoid arthritis: Auranofin. *Am. J. Med.* (**suppl 7A**) **75**: 69–73 (1983).
6. Wilke W. S, (editor). *Methotrexate Therapy In Rheumatic Diseases:* Marcel Dekker, New York (1989).
7. M. E. Weinblatt. *J. Rheumatol.* **12** (**suppl.**):35–39 (1985).
8. E. W. St. Clair, J. R. Rice, and R. Snyderman. *Arch. Intern. Med.* **145**:2034–2038 (1985).
9. R. Rau and T. Karger. *Arthritis Rheum.* **19**:S76 (1986).
10. G. S. Alarcon, I. C. Tracy, W. D. Blackburn Jr. *Arthritis Rheum.* **32**:671–676 (1989).
11. P. J. Brooks, W. J. Spruill, P. C. Roy, and D. A. Birchmore. *Arthritis Rheum.* **33**:91–94 (1990).
12. M. A. Ball, J. L. McCullough, and G. D. Weinstien. *J. Invest. Dermatol.* **79**:7–10 (1982).
13. G. D. Weinstien and J. Velasco. *J. Invest. Dermatol.* **59**:121–127.
14. L. Biro, R. Carriere, L. Frank, S. Minkowitz, and P. Petrou. *J. Invest. Dermatol.* **48**:429–437.
15. S. M Wallace, J. O. Runikus, and W. D. Stewart. *Can. J. Pharm. Sci.* **13**:66–68 (1978).
16. J. L. McCullough, D. S. Snyder, G. D. Weinstien, A. Friedland, and B. Stein. *J. Invest. Dermatol.* **66**:103–107 (1976)
17. J. J Fort, Z. Shao, A. K. Mitra. *Int. J. Pharm.* **100**:233–239 (1993).
18. O. Siddiqui, M. S. Roberts, and A. E. Polack. *Int. J. Pharm.* **27**:193–203 (1985).
19. K. R. Brian. *Int. J. Pharm.* **71**:R9 (1991).
20. B. J. Aungst, J. A. Blake, and M. A. Hussain. *Pharm. Res.* **7**:712–718 (1990).

21. K. J. Skeith, C. Ramos-Remus, and A. S. Russell. *J. Rheumatol.* **21**:473–475 (1994).
22. R. A. Herman, P. Veng-Pederson, J. Hoffman, R. Koehnke, and D. E. Furst. *J. Pharm. Sci.* **78**:165–171 (1989).
23. Furst D. E. *J. Rheumatol.* **12**:(suppl 12) 11–14 (1985).
24. M. J. Sinnet, G. D. Groff, D. A. Raddatz, W. A. Franck, and J. S. Bertino. *J. Rheumatol.* **16**:745–748 (1989).
25. D. J. Chatterjee. Doctoral dissertation, University of Southern California (1996).
26. L. F. Montes, J. L. Day, C. J. Wand, and L. Kennedy. *J. Invest. Dermatol.* **48**:184–187 (1967).
27. W. B. Barry. *J. Control. Rel.* **6**:85 (1987).
28. M. Goodman and B. W. Barry. In Bronaugh R. L. and Maibach H. I. (eds.), *Percutaneous Absorption,* Marcel Dekker, New York, 1989, chap. 33.
29. H. Okamoto, K. Muta, M. Hashida, and H. Sezaki. *Pharm. Res.* **7**:64 (1990).
30. R. Kadir and B. W. Barry. *Int. J. Pharm.* **70**:87 (1991).